An Investigation into the Electrical Impedance of Water Electrolysis Cells – With a View to Saving Energy

Kaveh Mazloomi[1,*], Nasri b. Sulaiman[1], Hossein Moayedi[2]

[1] Department of Electrical and Electronic Engineering, Faculty of Engineering, University Putra Malaysia
[2] Department of Civil Engineering, Estahban Branch, Islamic Azad University, Estahban, Iran
[*]E-mail: kavehoo@yahoo.com

Our research shows that the amount of power consumed in the production of electrolytic hydrogen can be reduced considerably by targeting the resonant frequency of the water electrolysis cell. We tested this by measuring the cell voltage for the same levels of current in both DC and frequency controlled pulsed voltage applications. In order to reach any given level of electrical current, a noticeable reduction of cell voltage was observed when the applied voltage was in the pulsed form at a certain frequency. Therefore, less power was applied to the cell in order to maintain its current level at a desirable value. Higher production efficiency was observed since the volume of produced hydrogen is a function of cell current. The amount of power consumption was up to 15% less in the frequency controlled pulsed voltage application mode. Aluminum plates with surface areas of 1.5 cm^2 and 10 cm^2 and potassium hydroxide aqueous solutions with molarities between 0.1 M and 2 M were used as electrode plates and electrolyte materials respectively. The electrode plates were placed in different distances ranging between 5 mm and 50 mm, and the power sources were sat to reach current densities between 50 mA and 400 mA. Random combinations of the mentioned variables were tested several times in order to study the electrical behavior, frequency response and impedance characteristics of the experimental cell setups.

1. INTRODUCTION

Hydrogen-based energy systems are known as promising replacements for conventional technologies [1-3]. Water electrolysis is meanwhile known to be one of the important assets for hydrogen production [4-9].

Enhancing the efficiency of water electrolysis is thus of considerable practical interest, as electricity expenses make up a large part of hydrogen production costs [3, 10, 11]. The required voltage value of an electrolysis cell is higher than the decomposition voltage of a water molecule. The excess voltage is known the overpotential of the cell [12-14].

Many efforts have been made to reduce the overpotential [4, 15-18] value for the water electrolysis process.

Research results show that temperature, pressure, electrode material, electrolyte formulation and concentration, physical setup of the cell and power supply output waveform have an influence on the value of the overpotential. Referring to Faraday's first law of electrolysis [19, 20], we know that "The local gas mass flow rate is proportional to the local current density". In other words: "The mass of a substance produced at an electrode during electrolysis is proportional to the number of moles of electrons (the quantity of electricity) transferred at that electrode". Hence, the goal of an energy efficient water electrolysis process is to reach higher levels of current while applying the minimum possible voltage to the cell. In most available literature, discussions on this subject are based on the physical and chemical configuration of an electrolytic bath rather than its electrical properties.

It is common to regulate the power or current of today's water electrolysis cells by controlling the output voltage level of a DC power supply [21-24] or by tuning the duty cycle of a pulse width modulator power driver [25-27]. These driving methods take no account of the impedance behavior of the electrolysis cell and are suitable for pure ohmic [28, 29] loads. At the same time, a few very similar electrical models have been introduced for electrolysis cells [14, 22, 30, 31]. By considering these models, it is possible to simplify the circuitry to a three component resistive-inductive-capacitive (RLC) circuit [32].

As well as any RLC circuitry, the minimum value of terminal to terminal impedance can be achieved by applying non-DC voltage to the cell at its natural frequency [33]. This consideration strongly suggests that there is scope for power saving in water electrolysis cells.

2. EXPERIMENTAL

The experimental water electrolysis cell is schematically illustrated in Figure 1. The cell consisted of a Pyrex container with a capacity of 1800 cm^3. Aluminum plate pairs with a thickness of 0.5 mm and surface areas of 1.5, 3, 6 and 10 cm^2 were placed at different distances of 0.5, 1 and 5 cm inside the cell.

Potassium hydroxide aqueous solutions with molarities of 0.1, 0.5, and 1 M played the role of electrolyte for the experiments. Cell temperature was maintained at 25 $\pm$ 2 °C during the tests by placing the experimental cell container in a water bath.

Two units of 0 to 30 V, 0 to 3 A laboratory DC power supplies were utilized in order to regulate the required voltage for the anode electrode. The power supplies had the ability to interconnect in parallel or series, or to function as separate stand-alone units. Different power supply configurations made it possible to reach a maximum voltage of 60 V or current level of 6000 mA.
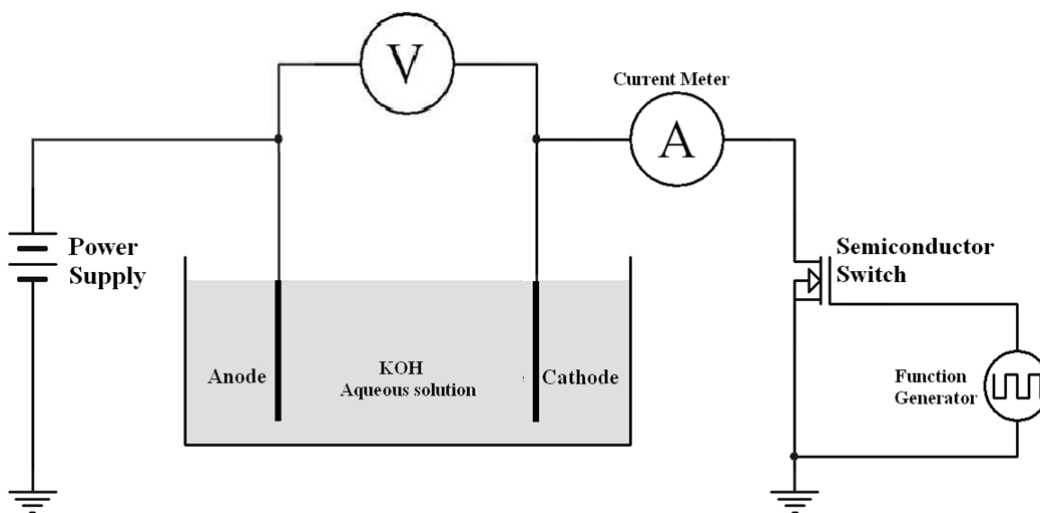
Figure 1. Experimental electrolysis cell

An ultra-low resistance metal oxide semiconductor field effect transistor (MOSFET) [34] was placed in the path of the cathode electrode and the electrical ground of the system. This device functioned as a switch which was able to conduct and cut off the current passing through the cell in the frequency range between 0Hz and 2 MHz. A high switching speed, low "ON state" voltage drop and ultra-low "OFF state" current leakage made it possible to assume the power MOSFET to be very close to an ideal switch [25]. The voltage drop and current leakage of the switching device were negligible due to its nominal ratings.

A laboratory electrical function generator was used to drive the power MOSFET. The latter was sat up to generate a square wave form with a duty cycle (ratio of on state to the total pulse period) of 50% - this is referred to as a pulse in this paper. The output frequency range of this device could be tuned between 0.1 Hz and 10 MHz. The amplitude of the generated signal was set at -0.5 V for shutdown and +18 V for turn-on commands in order to guarantee the best operational conditions for the semiconductor switch.

Laboratory voltage and current meters were used to read the DC voltage between the anode and cathode electrodes and the current passing through the cell. As the metering devices were unable to read accurate average values for non-DC signals with frequencies below 20 HZ due to their technical structure, those values were calculated mathematically [35] wherever they were required, although they are not vital to this research.

In order to study the frequency response of the cell, the first step of each experiment was to reach a level of current in DC voltage application mode. Random combinations of different electrode size, distance between electrodes and electrolyte molarities were set up for each test case. After applying a +18 V DC "ON" signal to the MOSFET, the output of the DC power supply was tuned to gain a desirable cell current.

Following the first step, the MOSFET driver signal was switched to square wave form. Cell voltage and current were read and stored as the frequency was changed on a logarithmic basis from 20

Hz to 2 MHz. The latter was done without changing the voltage of the power supply from the value of DC mode in each setup case. We repeated each experimental case 10 times in order to test the repeatability and reliability of the concept. The recorded data is used for further analysis in this paper.

In the next set of experiments, after finding the resonance frequency of each setup, the duty cycle of the electrical function generator was tuned to reach the same level of current as in the DC mode.

The power required to reach the same current density in both methods is analyzed in the sections that follow below.

3. RESULTS AND DISCUSSION

### 3.1. Frequency response of the cell

The available models of electrochemical cells suggest that water electrolysis baths have a non-linear impedance nature, although such systems are usually driven like ohmic loads. According to figures 2-5, the current versus frequency response of the experimental setups support the existence of a second order [32] equivalent circuit for modeling a cell. It should be mentioned that for an ohmic load, in the case of applying a pulsed signal with a duty cycle of 50% (which was used for all the experiments in this section), the average current is supposed to be half of the value of the time of DC voltage driving.

For instance, when a current level of 400mA is recorded in DC mode, a switching current value of 200mA is expected for pure resistive loads when the driving pulse duty cycle is 50%.

Figures 2 to 5 clearly show cell behavior as the switching frequency changes. The illustrated figures are a few samples to clarify the pattern of frequency responses of the experimental cells. The first graph of each figure represents the results of an individual test, whereas the second graph shows the maximum and minimum recorded values based on 10 tests for the experimental case.
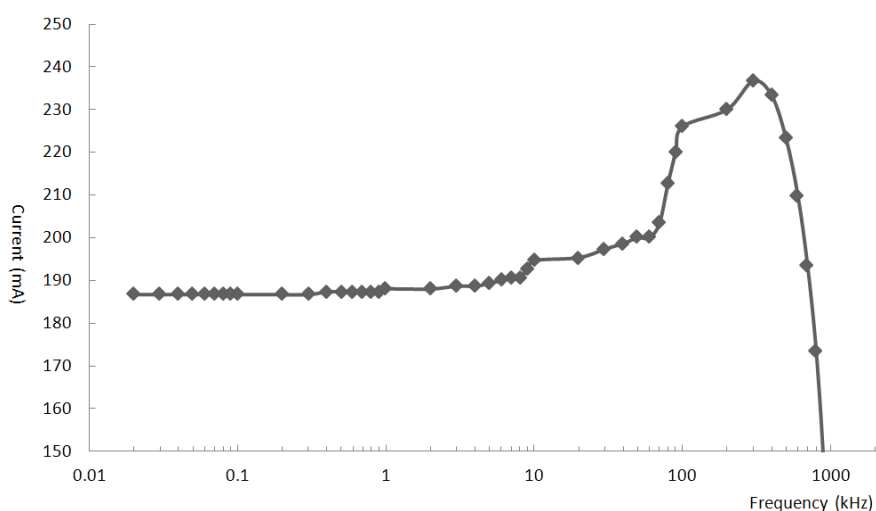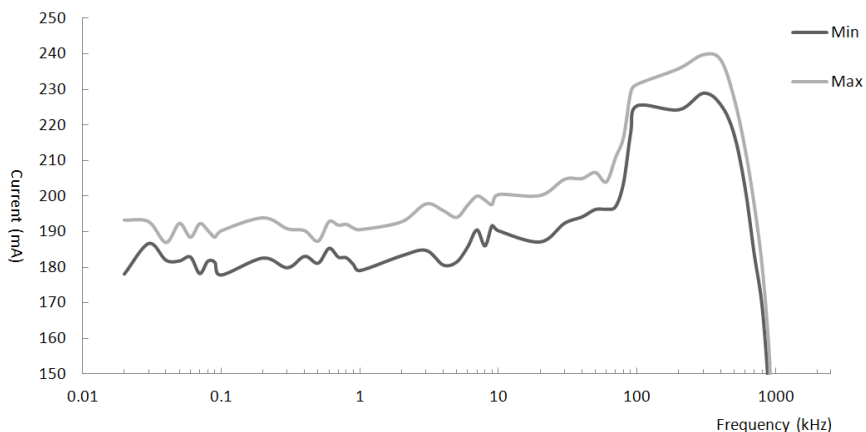
Figure 2. Current versus Frequency Graphs. (a) Sample cell current versus frequency for 1.5 cm^2 aluminum electrodes placed in 0.1M KOH solution at a 5 cm distance from each other. (b) Minimum and maximum recorded values based on 10 sets of recorded experimental results in the same conditions.
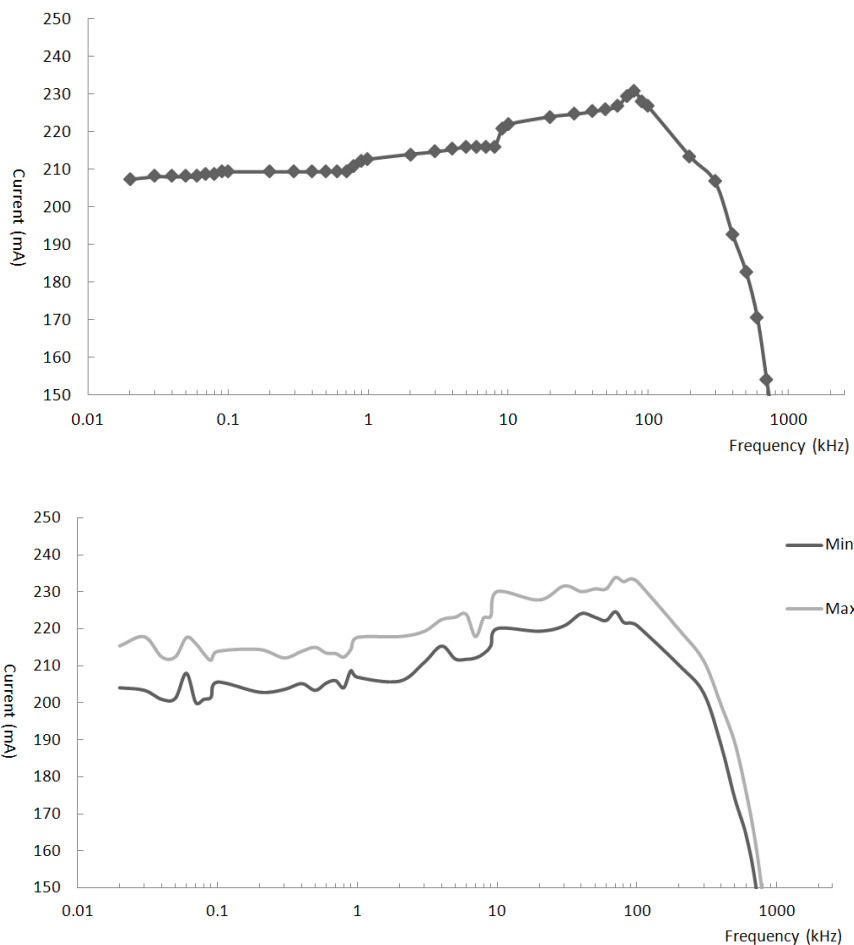

Figure 3b

Figure 3. Current versus Frequency Graphs. (a) Sample cell current versus frequency for 10 cm^2 aluminum electrodes placed in 0.1M KOH solution at 5 cm distance from each other. (b) Minimum and maximum recorded values based on 10 sets of recorded experimental results in the same conditions.

Figure 4. Current versus Frequency Graphs. (a) Sample cell current versus frequency for 1.5 cm^2 aluminum electrodes placed in 0.1M KOH solution at a 0.5 cm distance from each other. (b) Minimum and maximum recorded values based on 10 sets of recorded experimental results in the same conditions.
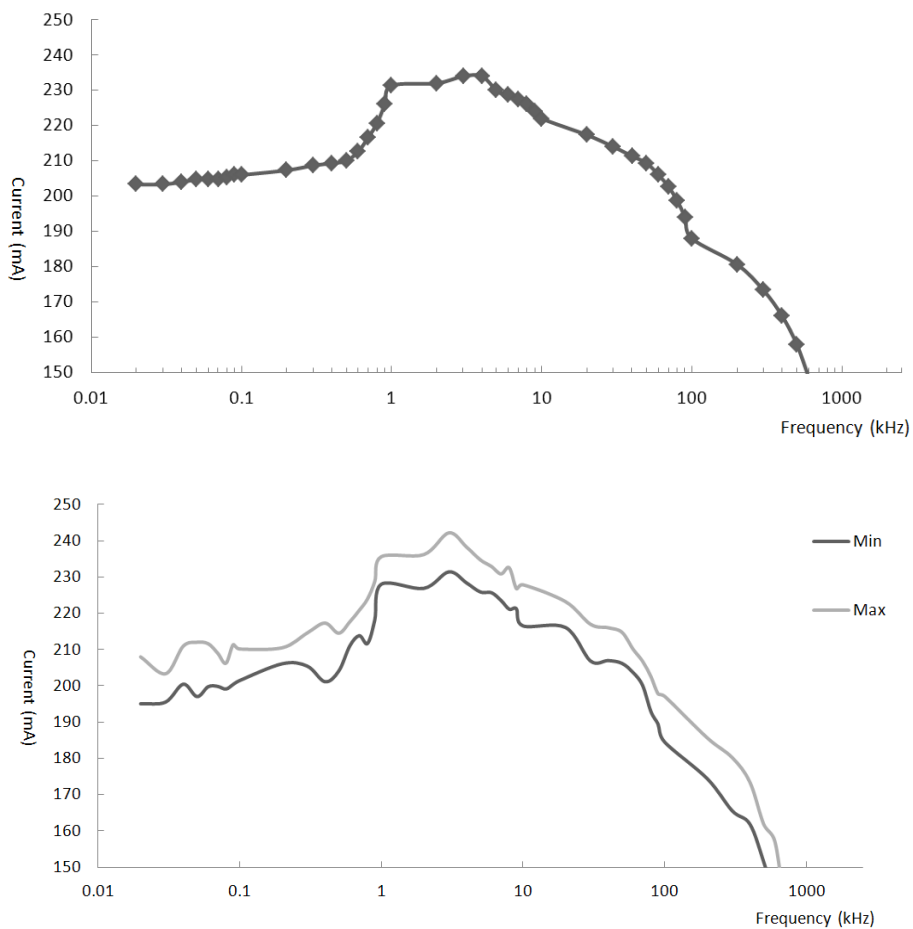
Figure 5. Current versus Frequency Graphs. (a) Sample cell current versus frequency for 1.5 cm^2 aluminum electrodes placed in 1M KOH solution at a 0.05 cm distance from each other. (b) Minimum and maximum recorded values based on 10 sets of recorded experimental results in the same conditions.
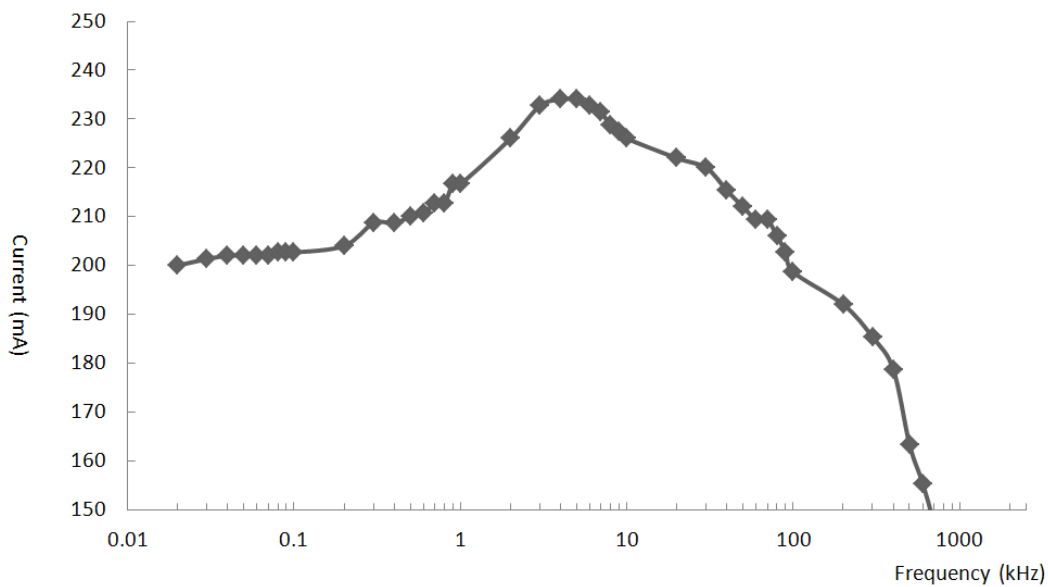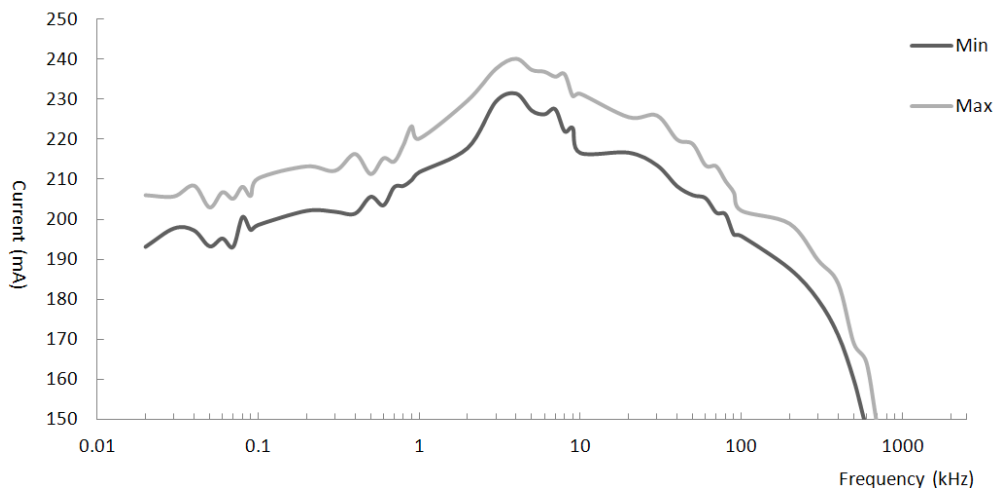
Table 1. summarizes the results of all tests. This table is based on the average value of each gathered data set.

Table 1. Natural frequency and peak currents for random setup cases

Electrode size (cm^2)	Distance between electrodes(cm)	Electrolyte molarity (M)	DC current (mA)	Natural frequency (kHz)	Peak current (mA)
1.5	0.5	0.1	400	600	236
1.5	0.5	1	400	20	232
1.5	1	0.1	400	600	243
1.5	1	1	400	40	240
1.5	1	1	200	50	138
1.5	5	0.1	400	200	230
1.5	5	0.5	200	4	141
3	0.5	0.1	50	300	29
3	0.5	0.1	100	600	67
3	0.5	0.1	200	700	136
3	5	0.1	200	200	127
3	5	1	100	20	61
3	5	1	50	5	29
6	0.5	0.1	400	200	241
6	0.5	1	200	20	135
6	1	0.5	400	50	239
6	1	0.1	200	10	131
6	5	0.1	400	500	232
6	5	0.1	200	30	119
10	0.5	0.1	400	20	228
10	0.5	0.5	200	2	117
10	5	1	1100	2	582
10	5	0.1	1100	0.4	565

3.2. Simplified equivalent circuit and impedance of the cell

The above mentioned results clearly follow the frequency response pattern of an RLC band pass circuit. Meanwhile, the simplified equivalent circuit of a capacitor is illustrated in Figure 6 [36].
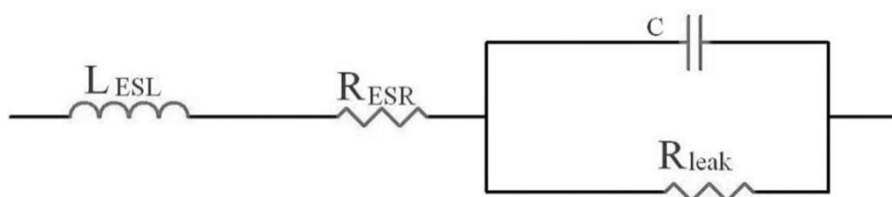

Figure 6. Equivalent circuit of a capacitor

Moreover a water electrolysis cell has structural similarities to an electrical capacitor as it is shown in Figure 7 schematically.
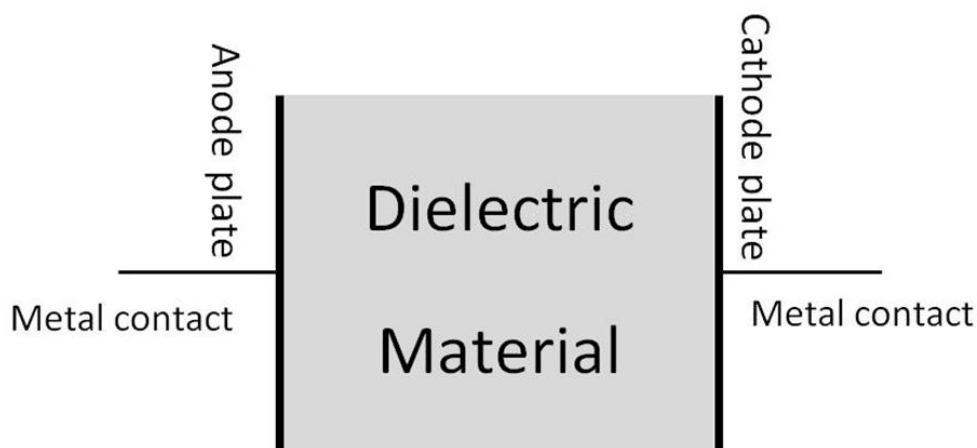
Figure 7. Structure of an electrical capacitor

As is clear from this schematic, a typical water electrolysis cell is composed of two parallel electrode plates, placed a certain distance from each other with the gap between them filled with an electrolyte. The existence of a level of insulation between the electrode plates is inevitable [37], although an electrolyte is generally meant to offer the minimum possible electrical resistance in order to conduct an efficient electrolysis process [12, 38]. Equation 1 shows the relation between the conductance *G* and resistance *R* of any given current path.

$$G = \frac{1}{R} \quad (1)$$

Adding ionic compounds to water is common in order to increase the conductivity of the electrolyte. This action causes the dielectric constant of the solution to be much less than with pure water [39-42]. However, even small values of dielectric constant can still exhibit a capacitive behavior in the cell. Capacitance is approximately calculable by equation 2[43].

$$C = \varepsilon_0 \, \varepsilon r \, \frac{S}{d} \quad (2)$$

Where C is the capacitance, $\varepsilon 0$ is the electric constant ($\approx 8.854 \times 10^{-12}$ Fm^{-1}), εr is the relative static permittivity (dielectric constant) of the material between the conductors, S is the overlap area of the conductor plates, and d is the distance between them.

Referring to Figure 6, the capacitance and resistance of the equivalent circuit are influenced by the internal setup of the cell, where the inductive element is mainly formed pursuant to the system wiring [44]. As in any RLC circuit, total circuit impedance is a function of frequency. In DC voltage application (f=0) the capacitor acts as an open circuit and the inductor as a short circuit. Equations 3 and 4 express the relative impedance of these elements:

$$Z_C = \frac{1}{2\pi f c} \quad (3)$$

$$Z_L = 2\pi f L \quad (4)$$

Where Z_C and Z_L are the impedances of the capacitor and inductor relatively, f is the frequency of the applied voltage, C is the capacitance of the capacitor and L is the inductance of the inductor.

Hence, the ohmic resistance of the electrolyte is the only influencing factor in the impedance of the cell, as it is not affected by frequency. As the frequency rises, the capacitor starts to conduct electrical current. It follows that the impedance of a model network can be calculated by Equation 5:

$$Z = Z_L + \frac{R.Zc}{R+Zc} \quad (5)$$

Where R is the resistance of the resistor. At higher frequencies, the network of parallel connected R and C values show lower equivalent impedance, although the impedance value of the inductor keeps rising slightly. Therefore, a rising current value is observed until the frequency reaches the natural value of the circuit. As the frequency tends to infinity (in analogy with the resonance frequency of the circuit), the equivalent impedance of the RC compartment tends to zero. Meanwhile the inductor starts to act as an open circuit and block the current path. As a result, the level of the current starts to fall as the frequency passes the resonance value. This slope does not change until the inductor cuts off the passing current completely.

Just like any RLC circuit, there is a natural frequency for the equivalent circuit, where the total impedance of the network reaches its minimum value. This frequency is obtained from Equation 6:

$$\omega_0 = \frac{1}{\sqrt{LC}} \qquad (6)$$

3.3. Energy saving

Where the electrical impedance of the cell can be minimized in this way, a lower cell voltage should be required in order to maintain the cell current at the desired value. This expectation is based simply on Ohm's Law [45], which can be expressed as Equation 7 where *V* is the voltage, *Z* is the electrical impedance, and *I* is the current passing through the cell:

$$V = ZI \qquad (7)$$

Our next step was to test the effect of adjusting the frequency of the applied voltage in order to enhance the efficiency of hydrogen production. In this test, the pulse width and the frequency of the applied signal were tuned simultaneously. At a certain pulse width, the frequency was manually varied to a higher or lower level. The value of the current of the cell was used as a guide to find out whether we were getting close to the natural frequency or not. Meanwhile, pulse width adjustments helped to maintain the target cell current density during the test. Cell voltage, current and current density were recorded at the resonance frequency for each cell configuration. By comparing the mentioned values as well as the cell power with those recorded in DC voltage mode, we were able to observe a reduction in the level of voltage and, as a result, of the level of power needed in order to achieve a certain level of current. The reduction of power required in order to maintain a given current level was considerable in the cases of high current density and larger electrode surface area size. This series of tests was also carried out on random cell configurations and repeated 10 times for each case. Table 2 shows the average values of each test, where A is the electrode surface area, d is the distance between electrodes, J is the current density, V is the voltage and I is current. The tests were conducted in potassium hydroxide with different molarities.

As it can be seen in table 2, the reported results are limited to the test cases in which the voltage readings did not exceed 20 V. We know that in order to maintain the current density level of the cell for larger electrode plates, its current has to be increase accordingly by tuning the level of applied voltage to the cell in this case. The mentioned limitation is because voltage tuning was the method of current regulation in the experimental work and since the utilized precision voltage-meter was unable to read the voltages over 20 V with the same resolution (10 mV) as those with the values below that barrier due to its internal and built limitations.

The mentioned voltage level fluctuations can be traced for different experimental cases reported in table 2. By reviewing table 2 it can be seen that the test conditions of each two consequent cases differ in only one variable. By comparing the results of the cases where the difference is the electrodes surface area, higher current level and as a result higher cell voltage is recorded. Meanwhile, increasing and decreasing the distance between electrodes caused higher and lower cell voltage levels respectively. Moreover, the use of more concentrated electrolyte solution resulted in lower electric resistance through the current path as its "specific electrical resistance" is lowered. The latter caused a

sudden reduction of inter-electrode voltage. These variations and their causes are explained more detailed as in equations 10 and 11 and figure 8.

Table 2. Cell voltage and current in DC and resonance mode

Cell Setup Conditions	Target J (mA cm^{-2})	I$_{cell DC}$ (mA)	V$_{cell DC}$ (V)	V$_{cell}$ resonant (V)	I$_{cell resonance}$ (mA)
A=1.5 cm^2 d= 10mm 0.1M KOH	50	75	6.05	5.75	75
	100	150	9.81	9.42	150
	200	300	15.49	15.25	300
A= 6 cm^2 d= 10mm 0.1M KOH	50	300	11.27	10.97	300
	100	600	17.73	17.19	600
A= 6 cm^2 d= 5mm 0.1M KOH	50	300	9.04	8.58	300
	100	600	12.47	12.08	600
A= 10 cm^2 d= 5mm 0.1M KOH	50	500	11.56	11.07	500
	100	1000	16.00	14.6	1000
A= 10 cm^2 d= 5mm 0.2M KOH	50	500	3.98	3.95	500
	100	1000	4.57	4.50	1000
	200	2000	6.74	6.09	2000
	300	3000	7.56	7.51	3000
A= 10 cm^2 d= 10mm 0.2M KOH	50	500	5.34	4.27	500
	100	1000	6.32	6.29	1000
	200	2000	7.90	7.80	2000
	300	3000	10.91	10.63	3000

As can be seen from Table 2, in all cases the desirable current density was reached with a lower cell average voltage; in other words, by consuming less power in resonance frequency than in DC mode. Cell power can be calculated by Equation 8 below:

$$P=V I \qquad (8)$$

Where **P** is cell power, **V** is cell average voltage and **I** is the average current level of the cell. Based on the observed reduced power application to the cell, a variable frequency pulse width modulated power driver could be used as a voltage, current or power regulator to drive an electrolytic hydrogen production unit.

According to the Faraday's laws of electrolysis, the mass of altered material at the surface of each electrode depends on the number of electrons passing through the cell. The volume of electrolytic gas production can be stated as in equation 9:

$$V = \frac{RITt}{Fpz} \qquad (9)$$

Where V is the volume of generated gas in liters, R is the ideal gas constant (=0.0820577 L atm mol^{-1} K^{-1}), I is the current in Amperes, T is the temperature in Kelvins, t is the time in seconds, F is the Faraday's constant (=96485.31 C mol^{-1}), p is the ambient pressure in atmospheres, and z is the number of excess electrons (=2 for H_2). As it can be seen, cell voltage does not have any effect on the amount of the produced gas.

As the cell temperature and pressure were the same for each and every test, cell current was the only changing value of the experiments.

As it is illustrated in table 2, application of the frequency controlled pulsed voltage causes less power consumption in order to maintain the cell current level at a certain level. Therefore, we observed higher hydrogen generation efficiency.

3.4. Equivalent circuit variables

As mentioned earlier, the assumed equivalent electrical circuit consists of resistive, capacitive and inductive elements. The values of, and influencing factors on, these are discussed separately below:

1- Resistive element: Is a result of the electrical resistance between electrode plates. The leakage resistor in the equivalent circuit of an actual capacitor causes the flow of unwanted currents through the dielectric medium between the plates. The electrical resistance of an electrolyte material can be calculated as in Equation 10:

$$R = \frac{\rho l}{A} \qquad (10)$$

Where R is the electrical resistance, ρ is the resistivity (specific electrical resistance) of the material, l is the length and A is the cross section area of the conductor. The value of leakage resistance between practical capacitor plates is usually very large because of the high levels of insulation generally found in common dielectric materials.

The resistance of the electrolyte ($R_{leakage}$) can be calculated by Equation 10 before the voltage is applied. The flow of electrical current forms gas bubbles in the electrolyte, which leads to the creation of a void fraction [46] between electrodes and a consequent reduction of the effective cross section area of the electric current path in that area. As is illustrated in Figure 8, the distance between electrodes "l" has been broken into n smaller segments "l_i". Hence, by using Equation 10, the resistance of each partial length of l_i section can be calculated.
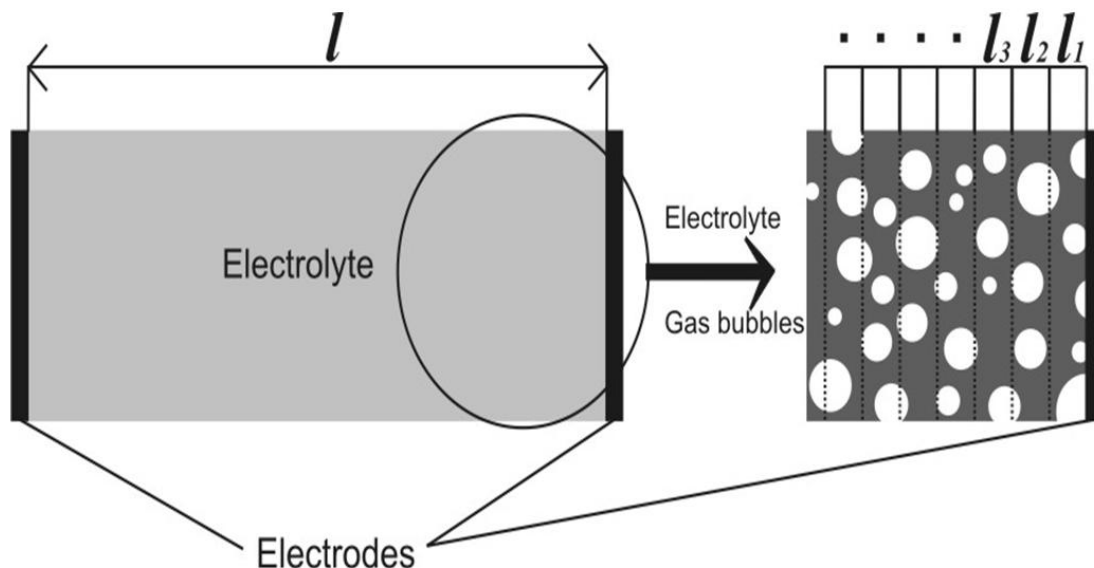
Figure 8. Void fraction formation in an electrolyte

As the efficient cross section area for each l_i is reduced by the presence of gas bubbles, the total amount of R increases. Hence, Equation 10 can be re-written as below:

$$R = \frac{\rho}{A}\left(\sum l_i\right) \qquad (11)$$

In addition, void fractions and bubble sizes are known to be affected by temperature and pressure respectively [47]. The rate at which bubbles form, their size and their departure speed in a water electrolysis cell is dependent on a number of factors, namely: the electric current density, the electrodes and separator materials, their size, shape and proximity, pressure, electrolyte molarity and any contaminations [12, 47-50]. After applying the voltage, any changes in the above-mentioned variables affect the void fraction value of the cell.

The value of the equivalent series resistance (R_{ESR}) is determined by the external electrical resistance values of the cell, such as the resistance of wiring and connections. This variable is affected by ambient circumstances such as temperature and wiring length.

2- Capacitive element: In addition to the capacitive nature of a water electrolysis cell discussed in prior sections, it should be mentioned that, although the dielectric constants of electrolytes are not as high as those of capacitors, a practical hydrogen production bath contains electrodes much larger than actual capacitor plates. Hence, its total capacitance is not negligible.

Moreover, the void fraction affects the dielectric constant of the mixture between electrode plates, as oxygen and hydrogen bubbles have dielectric constant values of their own. Hence, the capacitance of a water electrolysis cell is also a time variant function of the same influencing variables as leakage resistance.

3- Inductive element: Is the summation of the inductances of wiring, connections and intrinsic electrochemical inductances [44]. Therefore, the diameter, length, shape and temperature of wiring

have effects on the L_{ESL} − as do the applied voltage, frequency, electric current, connections method and electrolyte characteristics.

4. FURTHER WORKS

The value of each individual part of the introduced equivalent circuit is time variant. On the other hand, some can be represented as functions of the same physical variables. This makes introducing an exact mathematical model for the equivalent circuit a sophisticated task. This modeling could nevertheless help designers to make reasonably accurate assumptions when choosing or designing power regulation equipment for electrolysis systems. We therefore believe that mathematical modeling of the actual transfer function might be an interesting subject for further research.

In addition, further work to build and analyze experimental results based on numerous test cases is in our view recommended in order to point out relating patterns between the physical setup and frequency response of cells.

5. CONCLUSION

Driving a water electrolysis cell based on its natural frequency enhances the efficiency of hydrogen production. According to current vs. frequency graphs, an electrolysis cell shows minimal electrical impedance in its resonant frequency. This feature was used by us to reduce the cell voltage needed to reach a certain level of current. We were able to achieve a reduction in cell voltage of up to 15% in the cases of high current density and larger electrode surface area.

The concept of this research can be applied *mutatis mutandis* to any electrolysis cell, as the electrical equivalent circuits of these cells all follow similar patterns. However, the actual circuitry involved will not always be the same, as any physical setup change in the cell can lead to different element values in the equivalent circuits. This variation could in turn cause drifts in the natural frequency of the cell − although we would not expect these to have any significant impact on the level of voltage reduction or its value.

References

1. Seth Dunn. *Int. J. Hydrogen Energy*, 8 (2002) 16.
2. H. Balat and E. Kirtay. *Int. J. Hydrogen Energy*, 35 (2010) 7416.
3. A. Züttel, A. Borgschulte and L. Schlapbach, *Hydrogen as a Future Energy Carrier.* Darmstadt: Vch Verlagsgesellschaft Mbh, 2008.
4. S. Li, C. Wang and C. Chen, *Electrochim. Acta,* 54 (2009) 3877.
5. C. Gabrielli, F. Huet and R. P. Nogueira, *Electrochim. Acta,* 50 (2005) 3726.
6. S. A. Guelcher, Y. E. Solomentsev, P. J. Sides and J. L. Anderson, *J. Electrochem. Soc.,*145 (1998) 1848.

7. H. Matsushima, T. Nishida, Y. Konishi, Y. Fukunaka, Y. Ito and K. Kuribayashi, *Electrochim. Acta,* 48 (2003) 4119.
8. G. F. Naterer, M. Fowler, J. Cotton and K. Gabriel, *Int J Hydrogen Energy,* 33 (2008) 6849.
9. F. Gutiérrez-Martín, D. Confente and I. Guerra, *Int J Hydrogen Energy,* 35 (2010) 7329.
10. J. Ivy, "Summery of electrolytic hydrogen production: Milestone completion report, NREL/MP-560–36734," National Renewable Energy Laboratory, USA, Tech. Rep. NREL/MP-560–36734, Sep 2004.
11. B. Sorensen, *Renewable Energy. its Physics, Engineering, use, Environmental Impacts, Economy and Planning Aspects.* Elsevier Science, 2004.
12. K. Zeng and D. Zhang, *Progress in Energy and Combustion Science,* 36 (2010) 307.
13. M. Wang, Z. Wang and Z. Guo, *Int J Hydrogen Energy,* 35 (2010) 3198.
14. M. E. Orazem and B. Tribollet, *Electrochemical Impedance Spectroscopy.* New Jersey: Wiley Online Library, 2008.
15. K. Oldham and J. Myland. (1993, Fundamentals of Electrochemical Science (1st ed.).
16. J. C. Ganley. International Journal of Hydrogen Energy, 34 (2009) 3604.
17. K. Onda, T. Kyakuno, K. Hattori and K. Ito, *J. Power Sources,* 132 (2004) 64.
18. N. Shimizu, S. Hotta, T. Sekiya and O. Oda, *J. Appl. Electrochem.,* 36 (2006) 419.
19. J. O. Bockris and T. N. Veziroglu, *Int J Hydrogen Energy,* 32 (2007) 1605.
20. M. Philippe, H. Jérôme, B. Sebastien and P. Gérard, *Electrochim. Acta,* 51 (2005) 1140.
21. H. Wendt and G. Kreysa, *Electrochemical Engineering: Science and Technology in Chemical and Other Industries.* Springer Verlag, 1999.
22. Brad A.J., *Electrochemical Methods-Fundamentals and Applications.* New York: John Wiley, 1980.
23. J. Rossmeisl, A. Logadottir and J. K. Nørskov, *Chem. Phys.,* 319 (2005) 178.
24. Bockris JOM, Conway BE, Yeager E and White RE. Comprehensive Treatise of Electrochemistry. New York: Plenum Press, 1981.
25. A. I. '. 'Pressman, K. H. '. 'Billings and T. '. 'Morey, *Switching Power Supply Design.* USA: Mc Graw Hill, 2009.
26. Billings K.H. Switchmode Power Supply Hanndbook. USA: Mc Graw Hill, 1989.
27. C. P. Henze, H. C. Martin and D. W. Parsley, "Zero-voltage switching in high frequency power converters using pulse width modulation," in *Applied Power Electronics Conference and Exposition, 1988. APEC '88. Conference Proceedings 1988., Third Annual IEEE,* (1988) 33.
28. D. Kiuchi, H. Matsushima, Y. Fukunaka and K. Kuribayashi, *J. Electrochem. Soc.,* 153 (2006) 138.
29. L. J. J. Janssen, J. J. M. Geraets, E. Barendrecht and S. D. J. v. Stralen, *Electrochim. Acta,* 27 (1982) 1207.
30. Ø. Ulleberg, *Int J Hydrogen Energy,* 28 (2003) 21.
31. R. D. Armstrong and M. Henderson, *J Electroanal Chem,* 39 (1972) 81.
32. C. A. Desoer and E. S. Kuh, Basic Circuit Theory. Tata McGraw-Hill, 1984.
33. K. K. S. Suresh, Electric Circuits and Networks (for Gtu). Pearson Education India, 2010.
34. I. Batarseh. The power MOSFET. in Power Electronics Handbook (Second Edition), Muhammad H. Rashid, Academic Press, (2007) 41.
35. A. V. Oppenheim and A. S. Willsky, "Signals and Systems," 1983.
36. B. Somanathan Nair, Electronic Devices and Applications. New Delhi: Prentice-Hall, of India, 2006.
37. W. Benenson, J. W. Harris, H. Stocker and H. Lutz, Handbook of Physics. Springer, 2002.
38. R. L. LeRoy, *Int J Hydrogen Energy,* 8 (1983) 401.
39. J. B. Hasted, D. M. Ritson and C. H. Collie, *J. Chem. Phys.,* 16 (1948) 1.
40. National Research Council of the United States Of America. (2003, International Critical Tables of Numerical Data, Physics, Chemistry and Technology (1st electronic edition ed.) .
41. W. M. Haynes, *CRC Handbook of Chemistry and Physics.* Boca Raton, FL: CRC Press, 2010.

42. D. R. Lide, Handbook of Chemistry and Physics. CRC Press Inc, 2000.
43. D. K. Cheng, Fundamentals of Engineering Electromagnetics. Addison-Wesley, 1993.
44. B. Savova-Stoynov and Z. B. Stoynov, *J. Appl. Electrochem.,* 17 (1987) 1150.
45. P. Horowitz and W. Hill, The Art of Electronics. Cambridge university press, 2006.
46. N. Nagai, M. Takeuchi, T. Kimura and T. Oka, *Int J Hydrogen Energy,* 28 (2003) 35.
47. A. J. Appleby, G. Crepy and J. Jacquelin, *Int J Hydrogen Energy,* 3 (1978) 21.
48. H. Vogt, *Electrochim. Acta,* 34 (1989) 1429.
49. H. B. Suffredini, J. L. Cerne, F. C. Crnkovic, S. A. S. Machado and L. A. Avaca, *Int J Hydrogen Energy,* 25 (2000) 415.
50. Renaud and R. L. LeRoy, *Int J Hydrogen Energy,* 7 (1982) 155.